

# Unfolding the relationship between seasonal forecasts skill and value in hydropower production: A global analysis

Donghoon Lee<sup>1</sup>, Jia Yi Ng<sup>2</sup>, Stefano Galelli<sup>2</sup>, and Paul Block<sup>1</sup>

<sup>1</sup>University of Wisconsin-Madison

<sup>2</sup>Singapore University of Technology and Design

November 24, 2022

## Abstract

The potential benefits of seasonal streamflow forecasts for the hydropower sector have been evaluated for several basins across the world, but with contrasting conclusions on expected hydropower production and economic gains. This raises the prospect of a complex relationship between reservoir characteristics, forecast skill and value. Here, we unfold the nature of this relationship by studying time series of simulated power production for 735 headwater dams worldwide. The time series are generated by running a detailed dam model over the period 1958-2000 with three operating schemes: basic control rules, perfect forecast-informed, and realistic forecast-informed. The realistic forecasts are issued by bespoke models, based on lagged global and local hydroclimatic variables, predicting seasonal monthly dam inflows. Results show that most dams (94%) could benefit from perfect forecasts. Yet, the benefits for each dam vary greatly and are primarily controlled by the time to fill and the ratio between reservoir depth and hydraulic head. When realistic forecasts are adopted, 25% of dams demonstrate improvements with respect to basic control rules. In this case, the likelihood of observing improvements is controlled not only by design characteristics but also by forecast skill. We conclude our analysis by identifying two groups of dams of particular interest: dams that fall in regions expressing strong forecast accuracy and have the potential to reap benefits from forecast-informed operations, and dams with strong potential to benefit from forecast-informed operations but lack forecast accuracy. Overall, these results represent a first qualitative step towards informing site-specific hydropower studies.

1     **Unfolding the relationship between seasonal forecasts**  
2     **skill and value in hydropower production: A global**  
3     **analysis**

4     **Donghoon Lee<sup>1</sup>, Jia Yi Ng<sup>2</sup>, Stefano Galelli<sup>2</sup>, and Paul Block<sup>1</sup>**

5     <sup>1</sup>Department of Civil and Environmental Engineering, University of Wisconsin-Madison, Madison,  
6     Wisconsin, USA

7     <sup>2</sup>Pillar of Engineering Systems and Design, Singapore University of Technology and Design, Singapore

8     **Key Points:**

- 9     • 25% of the 735 headwater hydropower dams evaluated worldwide may benefit from  
10     seasonal forecasts conditioned on hydroclimatic predictors.
- 11    • Potential benefits are predominantly modulated by forecast skill and reservoir char-  
12     acteristics.
- 13    • We identify geographical regions where dams would benefit the most from fore-  
14     casts

**15 Abstract**

16 The potential benefits of seasonal streamflow forecasts for the hydropower sector have  
17 been evaluated for several basins across the world, but with contrasting conclusions on  
18 expected hydropower production and economic gains. This raises the prospect of a com-  
19 plex relationship between reservoir characteristics, forecast skill and value. Here, we un-  
20 fold the nature of this relationship by studying time series of simulated power produc-  
21 tion for 735 headwater dams worldwide. The time series are generated by running a de-  
22 tailed dam model over the period 1958-2000 with three operating schemes: basic con-  
23 trol rules, perfect forecast-informed, and realistic forecast-informed. The realistic fore-  
24 casts are issued by bespoke models, based on lagged global and local hydroclimatic vari-  
25 ables, predicting seasonal monthly dam inflows. Results show that most dams (94%) could  
26 benefit from perfect forecasts. Yet, the benefits for each dam vary greatly and are pri-  
27 marily controlled by the time to fill and the ratio between reservoir depth and hydraulic  
28 head. When realistic forecasts are adopted, 25% of dams demonstrate improvements with  
29 respect to basic control rules. In this case, the likelihood of observing improvements is  
30 controlled not only by design characteristics but also by forecast skill. We conclude our  
31 analysis by identifying two groups of dams of particular interest: dams that fall in re-  
32 gions expressing strong forecast accuracy and have the potential to reap benefits from  
33 forecast-informed operations, and dams with strong potential to benefit from forecast-  
34 informed operations but lack forecast accuracy. Overall, these results represent a first  
35 qualitative step towards informing site-specific hydropower studies.

**36 Plain Language Summary**

37 Seasonal streamflow forecasts are an important asset for hydropower operators. Their  
38 value has been assessed in several regions, but with contrasting conclusions on how pre-  
39 dictive accuracy, or skill, and dam design specifications affect the expected increase in  
40 power production. Here, we discover the nature of this relationship by studying a large  
41 dataset comprising seasonal forecasts and simulated hydropower production for 735 head-  
42 water dams worldwide, representing 10% of the world's installed hydropower capacity.  
43 Our results show that 25% of these dams demonstrate improvements. We conclude the  
44 analysis by identifying the values of forecast skill and design specifications that are nec-  
45 essary to reap immediate benefits from forecast-informed operations. Overall, the infor-  
46 mation revealed by this study could support the design and operations of large-scale hy-  
47 dropower projects.

## 48 1 Introduction

49 Hydropower is the leading form of renewable power, contributing to 16% of global  
50 electricity production and supplying 62% of all renewable electricity (IHA, 2019). To-  
51 tal hydropower generation is expected to double by 2050, with substantial growth in Asia,  
52 Africa, and South America (Zarfl et al., 2015; X. Zhang et al., 2018). Sustainable op-  
53 erations of hydropower facilities, however, are challenged by climate variability and change,  
54 which modify short-term and long-term water availability, often with direct effects on  
55 regional and global economies (Turner, Hejazi, et al., 2017).

56 Many studies assessed the potential impacts of climate change on global, continen-  
57 tal, and regional hydropower production using projected streamflow from hydrological  
58 models (Hamududu & Killingtveit, 2012; Van Vliet et al., 2016; Turner, Ng, & Galelli,  
59 2017; X. Zhang et al., 2018). For example, T. Zhou et al. (2018) outlines expected sub-  
60 stantial seasonal changes in hydropower generation in the western United States, while  
61 Kao et al. (2015) estimates that the United States federal hydropower production will  
62 decrease 1-2 TWh per year until 2039. Decreases in hydropower production in the late  
63 21<sup>th</sup> century are also expected in Europe (Lehner et al., 2005) and China (Liu et al., 2016),  
64 although regional variations are likely. Such projections in hydropower production can  
65 prompt policymakers to engage in strategic adaptation, including infrastructure expan-  
66 sion or alternative reservoir operating policies, to ensure water-energy security in the long  
67 run (Payne et al., 2004; Van Vliet et al., 2016).

68 In contrast to climate change, climate variability presents a fundamentally differ-  
69 ent challenge, namely seasonal and inter-annual fluctuations in streamflow and hydropower  
70 output driven by large-scale climate drivers. Examples include the North Atlantic Os-  
71 cillation (NAO), affecting hydropower in Europe (De Felice et al., 2018), and the El Niño  
72 Southern Oscillation (ENSO), affecting one third of the world’s hydropower dams (Ng  
73 et al., 2017). In theory, the negative impact of climate variability on hydropower pro-  
74 duction can be tackled with adaptive reservoir operating policies based on seasonal stream-  
75 flow forecasts, but, in practice, the ripped benefits depend on the complex relationship  
76 between hydropower production, forecast skill, and reservoir characteristics.

77 In previous studies, this relationship has been studied with either analytical or ex-  
78 perimental approaches. In the analytical approach, one typically uses synthetic forecasts  
79 and hypothetical reservoir systems (e.g., concave objective function, monotonic relation-  
80 ship between current operation decision and ending storage) to analytically derive a re-  
81 lationship between the aforementioned variables. For example, You and Cai (2008) de-  
82 rive a theoretical relationship linking the ideal forecast horizon to various factors, such

83 as water stress level, reservoir size, or inflow uncertainty. In a follow-up study, Zhao et  
84 al. (2012) investigate the relationship between forecast horizon and uncertainty, iden-  
85 tifying an effective forecast horizon that balances the effects of horizon and uncertainty,  
86 providing the largest benefit to the reservoir operators. In contrast, the experimental ap-  
87 proach simulates the operations of existing reservoirs systems with seasonal streamflow  
88 forecasts to determine their potential value—and, where possible, to build an empirical  
89 relationship linking forecast value, skill, and reservoir characteristics. A common, and  
90 expected, conclusion shared by many studies is that incorporating streamflow forecasts  
91 into reservoir operating policies can lead to increased hydropower production and eco-  
92 nomic gains (Kim & Palmer, 1997; Ahmad & Hossain, 2019). What is perhaps more in-  
93 teresting is that the expected gains vary widely. Maurer and Lettenmaier (2004), for in-  
94 stance, observed a modest 1.8% hydropower benefit for reservoirs along the Missouri River  
95 utilizing perfect forecasts. They attribute the relatively low gains to the system’s large  
96 storage capacity relative to annual inflow. Similarly, Rheinheimer et al. (2016) noted an  
97 expected 1.2% economic gain for hydropower systems in the Sierra Nevada (California)  
98 and found that forecast value is insensitive to storage capacity, yet highly sensitive to  
99 powerhouse capacity. By contrast, Hamlet et al. (2002) used ENSO and the Pacific Decadal  
100 Oscillation (PDO) signals to construct long-range streamflow forecasts, and estimated  
101 that such forecasts could increase hydropower revenue by \$153 million/year ( $> 40\%$ ) for  
102 the Columbia River system. Recently, Anghileri et al. (2019) applied subseasonal hydrom-  
103 eteorological forecasts to improve both revenue and unproductive spill for the Verzasca  
104 hydropower system in the Swiss Alps. Similar benefits have been demonstrated in many  
105 other countries, such as Ecuador (Gelati et al., 2014), Ethiopia (Block, 2011), and the  
106 Philippines (Sankarasubramanian et al., 2009; Libisch-Lehner et al., 2019).

107 While these studies illustrate the potential benefits of seasonal forecasts, they are  
108 limited to individual dams or specific river basins. A ‘synoptic’ assessment of the value  
109 of seasonal forecasts for global hydropower production is lacking. In addition, there is  
110 only fragmented knowledge on how forecast skill and reservoir characteristics translate  
111 into forecast value. Characterizing such relationship across multiple geographic areas and  
112 climatic conditions may provide valuable insights for planning and managing hydropower  
113 projects. Here, we address these gaps by presenting a global analysis carried out on 753  
114 headwater dams, representing 10% of the world’s installed hydropower capacity. Specif-  
115 ically, we leverage recent studies demonstrating global streamflow predictability condi-  
116 tioned on large-scale climate variability (Ward et al., 2014; Lee et al., 2018) and develop  
117 seasonal inflow forecasts for each dam. Then, we quantify the value of these forecasts  
118 by comparing the amount of hydropower simulated by three operating schemes based  
119 on realistic forecasts (issued by our model), perfect forecasts, and (no forecasts) control

120 rules. With this information at hand, we bank on the wide range of climatic conditions  
121 and dam characteristics available in our database to (1) explain how reservoir design prop-  
122 erties and forecast skill affect the value of seasonal forecasts, and (2) identify key geo-  
123 graphical regions where dams would benefit the most from forecasts. As we shall see, the  
124 relationship (between forecast skill and value) and spatial patterns revealed by our anal-  
125 yses represent a first qualitative step towards informing site-specific studies.

## 126 **2 Data**

### 127 **2.1 Hydropower dams data**

128 We use the database introduced by Ng et al. (2017), which contains design spec-  
129 ifications for 1,593 hydropower reservoirs—representing almost 40% of the world’s in-  
130 stalled hydropower capacity. The database provides information on dam height, stor-  
131 age capacity, maximum surface area, long-term average discharge, upstream catchment  
132 area, geographic coordinates, installed power capacity, maximum turbine flow, and op-  
133 erating goals (e.g., hydropower supply, flood control). The majority of these data were  
134 originally retrieved from the Global and Dam (GRanD) database (Lehner et al., 2011),  
135 and complemented with data from the International Commission on Large Dams (ICOLD,  
136 2011), the Global Lakes and Wetlands Database (Lehner & Döll, 2004), and the Global  
137 Energy Observatory (GEO, 2016). The fact that not all dams in the database are located  
138 in the headwaters is a major challenge, since the inflows are forecasted based on hydro-  
139 meteorological data only (see Section 3.1. For this reason, we filter out all dams affected  
140 by upstream regulation, reducing the number of dams from 1,593 to 753. To this pur-  
141 pose, we first retrieve data on the Degree Of Regulation (DOR) for each dam, defined  
142 as the ratio between the storage volume of the upstream dam(s) and the natural aver-  
143 age discharge volume of a given river segment (Grill et al., 2019). We then keep only the  
144 dams with DOR equal to 0.

145 To model the relationship between storage and depth, one ideally needs data on  
146 the bathymetry of each reservoir, an information not available at the global scale. Re-  
147 cent advances in remote sensing have shown that these data can be estimated from satel-  
148 lite images (Gao et al., 2012; Bonnema & Hossain, 2017), but for a number of reservoirs  
149 that is not yet compatible with the scale of our work (Busker et al., 2019). For this rea-  
150 son, we adopt a simpler bathymetry commonly adopted in global studies (Van Beek et  
151 al., 2011; Turner, Ng, & Galelli, 2017). Specifically, we model the storage-depth relation-  
152 ship with Kaveh’s method, which assumes an archetypal reservoir shape (Kaveh et al.,  
153 2013). This method estimates the reservoir surface area as a function of volume, max-  
154 imum surface area, depth, and maximum depth. For the limited number of cases in which

155 data on the maximum depth are not available, we adopt Liebe’s method, which assumes  
156 that a reservoir is shaped like an inverted pyramid cut diagonally in half (Liebe et al.,  
157 2005).

158 For each dam, we obtain a monthly inflow time series from the Water and Global  
159 Change (WATCH) 20<sup>th</sup> century model gridded global runoff dataset (Weedon et al., 2011).  
160 The runoff data are generated by the global hydrological model WaterGAP (Alcamo et  
161 al., 2003), which estimates the accumulated runoff for each grid ( $0.5^\circ \times 0.5^\circ$  resolution)  
162 using the DDM30 river network (Döll & Lehner, 2002). The model has found success-  
163 ful application in various global water resources studies (Döll et al., 2009; Haddeland et  
164 al., 2014), but its spatial resolution may be a source of uncertainty for dams located in  
165 small catchments. For this reason, we modify the original WATCH database in three ways.  
166 First, we consider only the period 1958–2000, which contains more detailed forcing data  
167 (Weedon et al., 2011). Second, we manually adjust the position of 270 dams (among the  
168 753 dams with DOR equal to 0) to properly align them with the DDM30 river network.  
169 To this purpose, we use the HydroSHEDS river network (Lehner et al., 2008) and satel-  
170 lite images. Lastly, we correct the discharge data to account for any disparity between  
171 the upstream catchment area defined by the DDM30 river network and the documented  
172 upstream catchment area of each dam (Ng et al., 2017).

173 In addition to the inflow time series, we also retrieve information on the climate  
174 classification of each dam location, an information needed in the latter part of our anal-  
175 ysis to characterize the regions that would benefit the most from forecasts. To this pur-  
176 pose, we use the updated Köppen-Geiger Climate classification developed on the basis  
177 of a large global data set of long-term monthly precipitation and temperature time se-  
178 ries (Peel et al., 2007). Specifically, we use the most frequent Köppen-Geiger Climate  
179 classification in all upstream grids for each dam.

## 180 **2.2 Hydro-climatological data**

181 The seasonal forecasts developed here depend on seven predictors: four large-scale  
182 climate drivers (ENSO, PDO, NAO, and Atlantic Multidecadal Oscillation (AMO)), and  
183 three variables accounting for local processes (lagged inflow, snowfall, and soil moisture.)  
184 The four large-scale climate drivers are interannual, decadal, or multidecadal quasiperi-  
185 odic oscillations derived from oceanic and atmospheric fields, and play a key role in de-  
186 termining climate patterns across the world. To characterize ENSO, we use the Niño 3.4  
187 index, defined as the anomalies of 3-month running mean of Sea Surface Temperature  
188 (SST) in the Niño 3.4 region ([https://www.esrl.noaa.gov/psd/gcos\\_wgsp/Timeseries/  
189 Nino34/](https://www.esrl.noaa.gov/psd/gcos_wgsp/Timeseries/Nino34/)). The monthly PDO index is defined as the leading principal component of monthly

190 SST anomalies in the North Pacific basin (Y. Zhang et al., 1997). It is obtained from  
191 the Joint Institute for the Study of the Atmosphere and Ocean (<http://research.jisao>  
192 [.washington.edu/pdo/](http://research.jisao.washington.edu/pdo/)). For NAO, we use the station-based seasonal NAO index, which  
193 is the difference in normalized sea level pressure between Reykjavik and Lisbon stations  
194 (Hurrell & Deser, 2010) (<https://climatedataguide.ucar.edu/climate-data/hurrell>  
195 [-north-atlantic-oscillation-nao-index-station-based](https://climatedataguide.ucar.edu/climate-data/hurrell-north-atlantic-oscillation-nao-index-station-based)). Finally, the AMO index  
196 is defined as the area-weighted average SST over the North Atlantic basin (Enfield et  
197 al., 2001). We use the monthly de-trended and un-smoothed AMO index derived from  
198 the Kaplan SST ([https://www.esrl.noaa.gov/psd/gcos\\_wgsp/Timeseries/AMO](https://www.esrl.noaa.gov/psd/gcos_wgsp/Timeseries/AMO)). For  
199 the PDO and AMO indices, we calculate the 3-month running mean to maintain sea-  
200 sonal persistence.

201 Monthly soil moisture and snowfall data are obtained from the ERA-40 reanaly-  
202 sis, developed by the European Centre for Medium-Range Weather Forecasts ([https://](https://apps.ecmwf.int/datasets/)  
203 [apps.ecmwf.int/datasets/](https://apps.ecmwf.int/datasets/)) and WATCH forcing data, respectively. For soil moisture,  
204 we aggregate all four volumetric soil water layers of the ERA-40. To properly account  
205 for the basin-scale soil moisture and snowfall states (Maurer & Lettenmaier, 2004), we  
206 calculate the area-weighted average soil moisture and snowfall of all upstream grids for  
207 each dam using the DDM30 river network.

### 208 **3 Methods**

209 The purpose of this study is to (1) quantify the value of seasonal inflow forecasts  
210 for global hydropower production, (2) explain how reservoir design properties and fore-  
211 cast skill affect the value of seasonal forecasts, and (3) identify regions that would ben-  
212 efit the most from seasonal forecasts. To achieve these goals, we first develop an inflow  
213 prediction model for each of the 753 dams (Section 3.1). Then, we simulate hydropower  
214 production for each dam under three operating schemes that are based on perfect fore-  
215 casts, realistic forecasts (issued by our inflow prediction model), and (no forecast) con-  
216 trol rules (Section 3.2). Finally, we evaluate the performance of each operating scheme  
217 and identify the reservoir design specifications that explain system’s performance (Sec-  
218 tion 3.3).

#### 219 **3.1 Dam inflow prediction model**

220 Our long-range inflow prediction models are based upon the methodology presented  
221 by Lee et al. (2018), who employed lagged large-scale climate drivers and prior stream-  
222 flow conditions to predict streamflow at 1,200 stations globally. Lee et al. (2018) sug-  
223 gested that a Principal Component Regression (PCR) model with a set of predictors can

224 provide fair (realistic) predictive skills that can also be easily implemented globally. While  
 225 Lee et al. (2018) predicted the seasonal (3-month) streamflow, here we develop indepen-  
 226 dent monthly prediction (MP) models for the subsequent seven calendar months. For  
 227 example, at the end of February, we predict monthly inflows from March (MP1) to Septem-  
 228 ber (MP7).

229 The methodology relies on the following steps, illustrated in Figure 1. First, we nor-  
 230 malize (log-normalize for streamflow) and detrend all predictors and streamflow obser-  
 231 vations to avoid artificial skill due to potential dependence. Then, we estimate the lag-  
 232 correlations between monthly inflows over the next 7 months and climate indices (1-8  
 233 months ahead), snowfall (current to 8 months ahead), and inflow and soil moisture (cur-  
 234 rent month). Statistically significant predictors are subsequently used to develop the MP  
 235 models. If a single (statistically significant) predictor exists, we apply a linear regression  
 236 (LR) model; otherwise, we apply the PCR model to avoid possible multicollinearities.  
 237 In the PCR process, we truncate only the last principal component, which is associated  
 238 with multicollinearities, as suggested by Jolliffe (2002) and Wilks (2011). We apply a  
 239 leave-one-out cross-validation (LOOCV) scheme to select the optimal lead-times of the  
 240 lagged predictors. Specifically, all combinations of lead months for the lagged predictors  
 241 are cross-validated with a block size of 3 years; then, the optimal set of lead-months is  
 242 determined based on the minimum mean squared error (MSE). The models are calibrated  
 243 with 70% of the available data (corresponding to the period 1958–1987) and validated  
 244 with the remaining data (1988–2000). In the validation process, we evaluate the model  
 245 performance using two skill scores, namely the mean squared error skill score (MSESS)  
 246 and the Gerrity skill score (GSS) (Appendix A), as in Lee et al. (2018). If an MP model  
 247 has no statistically significant predictors, or either an MSESS or GSS value less than 0,  
 248 the climatological mean prediction is used instead.

249 The overall accuracy of the reservoir inflow predictions is assessed with the Kling-  
 250 Gupta efficiency (*KGE*), which compares correlation, bias, and variability of the pre-  
 251 dicted and observed discharge (Gupta et al., 2009). The *KGE* is defined as:

$$KGE = 1 - \sqrt{(r - 1)^2 + (\beta - 1)^2 + (\gamma - 1)^2}, \quad (1)$$

252 where  $r$  is the correlation coefficient,  $\beta$  the bias ratio of the mean inflow ( $\mu_s/\mu_o$ ),  $\gamma$  the  
 253 variability ratio ( $CV_s/CV_o$ ),  $\mu$  the mean flow,  $CV$  the coefficient of variation, and  $s$  and  
 254  $o$  two indices indicating simulated (predicted) and observed inflow values, respectively.

255        **3.2 Reservoir operation model**

256        **3.2.1 Reservoir model**

257        An essential component of the operating schemes described below is the reservoir  
258 mass balance:

$$S_{t+1} = S_t + Q_t - E_t - R_t - Spill_t, \quad (2a)$$

$$0 \leq S_t \leq S_{cap}, \quad (2b)$$

$$0 \leq R_t \leq \min(S_t + Q_t - E_t, R_{max}), \quad (2c)$$

259        where  $S_t$  is the reservoir storage at month  $t$ ,  $Q_t$  the inflow volume (retrieved from the  
260 WaterGAP model, as described in Section 2.1),  $E_t$  the evaporation loss, and  $R_t$  the wa-  
261 ter released through the turbines. Both  $S_t$  and  $R_t$  are constrained by the reservoir de-  
262 sign specifications. Specifically, the storage cannot exceed the reservoir capacity  $S_{cap}$  (eq.  
263 (2b)), while the discharge is bounded by the water availability and capacity  $R_{max}$  of the  
264 turbines (eq. (2c)). Excess water, if any, is spilled:

$$Spill_t = \max(0, S_t + Q_t - R_t - E_t - S_{cap}). \quad (2d)$$

265        The hydropower production  $P_t$  (in MW) is calculated as follows:

$$P_t = \eta \cdot \rho \cdot g \cdot r_t \cdot h_t, \quad (3)$$

266        where  $\eta$  is the efficiency of the turbines assumed constant over the simulation period),  
267  $\rho$  the water density (1,000 kg/m<sup>3</sup>),  $g$  the gravitational acceleration (m/s<sup>2</sup>),  $r_t$  the aver-  
268 age release rate (m<sup>3</sup>/s) implied by the monthly release volume  $R_t$ , and  $h_t$  the hydraulic  
269 head (m). The latter is taken as the average head between time  $t$  and  $t + 1$ .

270        **3.2.2 Benchmark scheme: control rules**

271        Our benchmark operating scheme relies on the approach proposed by Ng et al. (2017),  
272 in which the behaviour of the hydropower operators is modelled as an optimal control  
273 problem. This approach builds on two main assumptions, on which we shall return in  
274 Section 5. First, the goal of the operators is to maximize hydropower production over

275 the long term. This objective provides a tangible indication of hydropower performance,  
 276 so it is commonly adopted in large-scale studies (e.g., Van Vliet et al. (2016)). Second,  
 277 the release decision  $R_t$  depends on the reservoir storage  $S_t$ , the previous period’s inflow  
 278 volume  $Q_{t-1}$ , and month of year  $t$ —a common choice in real-world reservoir operating  
 279 schemes (Hejazi et al., 2008). In other words, the approach assumes that each reservoir  
 280 is operated through a bespoke, periodic look-up table of turbine release decisions, which  
 281 is generated with stochastic dynamic programming (Loucks et al., 2005; Soncini-Sessa  
 282 et al., 2007). In the optimization, the inflow process is modelled with a first order, pe-  
 283 riodic Markov chain, whose parameterization is derived from the inflow data. A detailed  
 284 validation of the operating rules—based on values of observed hydropower production  
 285 in 107 countries during the period 1980–2000—is reported in Turner, Ng, and Galelli (2017).  
 286 The time series of all process variables (e.g., inflow, storage, release, hydropower produc-  
 287 tion) obtained by the benchmark control scheme are available on HydroShare ([http://](http://www.hydroshare.org/resource/ca365ffb1a1f49df8b77e393be965fd8)  
 288 [www.hydroshare.org/resource/ca365ffb1a1f49df8b77e393be965fd8](http://www.hydroshare.org/resource/ca365ffb1a1f49df8b77e393be965fd8)).

### 289 **3.2.3 Forecast-informed scheme**

290 To assess the value of seasonal streamflow forecasts, we adopt an adaptive scheme  
 291 based on the *receding horizon principle* (Bertsekas, 1976): at month  $t$ , we use a 7-month  
 292 streamflow forecast to determine the value of the release decisions for the next seven months,  
 293 and then implement only the decision  $R_t$  for the first month. At month  $t + 1$ , when a  
 294 new 7-month forecast becomes available, a new sequence of release decisions is determined.  
 295 Each decision-making process is formulated through an optimization problem that max-  
 296 imizes the hydropower production over the forecast horizon while accounting for the ben-  
 297 efits associated with the resulting storage at the end of the forecast horizon:

$$\min_{R_t, R_{t+1}, \dots, R_{t+6}} \sum_{i=0}^6 P_{t+i} + X(S_{t+7}) \quad (4)$$

298 where  $P_t$  is the hydropower production (see eq. (3)) and  $X(\cdot)$  a function accounting for  
 299 the long-term effect of the release decisions. Specifically, the function penalizes decisions  
 300 that solely optimize energy production in the short term, risking depleted water avail-  
 301 ability in the long term. Following a common practice in forecast-informed schemes (Soncini-  
 302 Sessa et al., 2007), we set  $X(\cdot)$  equal to the benefit function obtained by the benchmark  
 303 control rules, which contains information about the expected long-term hydropower pro-  
 304 duction for a given storage level. Thus, the real-time information provided by the fore-  
 305 casts may alter decisions otherwise based solely on the benchmark scheme (Turner, Ben-  
 306 nett, et al., 2017). The optimization problem is solved at each time step using determin-  
 307 istic dynamic programming [ibidem].

308 The scheme is implemented using both ‘perfect’ and realistic forecasts (described  
 309 in Section 3.1). Both benchmark and forecast-informed schemes are simulated over the  
 310 period 1958–2000. During the simulation, all release decisions are constrained to satisfy  
 311 downstream environmental flow requirements, calculated using the variable monthly flow  
 312 method (Pastor et al., 2014). All experiments are carried out with the R package *reser-*  
 313 *voir* (Turner & Galelli, 2016).

#### 314 **3.2.4 Dealing with additional operating objectives and finer temporal** 315 **scales**

316 Of the 735 dams, 174 dams within the database are also operated for flood con-  
 317 trol purposes. For these dams, we penalize spill to account for flood control and formu-  
 318 late the optimization objective as follows (in both benchmark and forecast-informed schemes):

$$\min \sum_t (w_1 \cdot \frac{Spill_t}{p_{95}(Q)} + w_2 \cdot (1 - \frac{P_t}{P})) \quad (5)$$

319 where  $w_1$  and  $w_2$  are the weights associated to the flood control and hydropower objec-  
 320 tives, set to 0.5 here,  $p_{95}(Q)$  the 95<sup>th</sup> percentile of the inflow time series  $Q$ , and  $P$  the  
 321 installed hydropower capacity (in MW). The presence of an additional goal may result  
 322 in a change of the hydraulic head or release trajectory, thereby affecting hydropower pro-  
 323 duction (Zeng et al., 2017).

324 A second modification of the reservoir operation model concerns the monthly decision-  
 325 making time step, which may not be suitable for reservoirs with small storage capacity  
 326 relative to inflow (or time-to-fill). We therefore identify a group of 94 reservoirs for which  
 327 the time-to-fill is smaller than two months, and adopt for this group only a weekly time  
 328 step. Since the inflow forecasts have a monthly resolution, we disaggregate each forecast  
 329 into four values using the  $k$ -nearest neighbors algorithm. Further details are reported  
 330 in Text S1.

### 331 **3.3 Reservoir performance evaluation**

332 The value of seasonal streamflow forecasts—here measured in terms of hydropower  
 333 production—certainly depends on predictive skill; however, a second important factor  
 334 influencing forecast value are the reservoir characteristics. For example, a reservoir con-  
 335 strained by small turbine capacity may perform adequately well utilizing control rules  
 336 alone as storage is sufficient to buffer inflow variability. Thus, we are not only interested  
 337 in quantifying forecast value, but also in understanding how value varies as a function  
 338 of both skill and reservoir characteristics.

339 **3.3.1 Impact of design characteristics for a perfect forecast-based ap-**  
 340 **proach**

341 Initially excluding the effect of actual forecast skill, the following performance met-  
 342 ric represents the expected improvement from perfect forecast-informed operations as  
 343 compared to control rules-based operations:

$$I_{PF} = \frac{H_{PF} - H_{ctrl}}{H_{PF}} \times 100\%, \quad (6)$$

344 where  $H_{PF}$  and  $H_{ctrl}$  represent the total hydropower production (for the period 1958–  
 345 2000) obtained with perfect forecast-informed operations and control rules, respectively.  
 346 A negative value indicates that the control rules outperform the (perfect) forecast-informed  
 347 operations, whereas a positive value suggests that forecast-informed operations could be  
 348 beneficial.

349 To understand how reservoir characteristics may influence benefits based on a per-  
 350 fect forecast approach, we proceed in two steps. First, we label each dam as *success* or  
 351 *failure* depending on whether the associated value of  $I_{PF}$  is larger or smaller than the  
 352 mean value of  $I_{PF}$  across all dams. Note that *failure* implies that the control rules and  
 353 (perfect) forecast-informed operations generate a similar amount of hydropower, and thus  
 354 storage and previous month inflow quantities are sufficient for near-optimal release de-  
 355 cisions. Second, we explain the likelihood of achieving success through a logistic regres-  
 356 sion model in which the probability of the binary response variable taking a particular  
 357 value is a function of the predictor variables. We consider two predictors, namely (1) the  
 358 ratio of reservoir storage capacity to the mean monthly inflow ( $x_{fill}$ , measured in months),  
 359 and (2) the ratio of maximum reservoir depth to maximum hydraulic head ( $x_{depth}$ ). The  
 360 second predictor varies between 0 and 1, and indicates the extent to which hydraulic head  
 361 is dependent on the depth of the reservoir. The logistic regression model is cross-validated  
 362 with a 10-fold cross-validation scheme, and evaluated using two metrics, accuracy and  
 363 Cohen’s kappa (McHugh, 2012). Accuracy is the ratio of correctly predicted observations  
 364 (true positives and true negatives) to the total number of observations. Cohen’s kappa  
 365 is an adjusted accuracy score that accounts for the possibility of correct predictions oc-  
 366 ccurring by chance. The modelling exercise is carried out with the R package *caret*. For  
 367 additional details, please refer to Text S2, and Table S1–S2 in the Supporting Informa-  
 368 tion.

369 **3.3.2 Impact of forecast skill and design characteristics for a realistic**  
 370 **forecast-based approach**

371 Integrating realistic forecasts in lieu of perfect forecast information, we introduce  
 372 the following performance metric:

$$I_{DF} = \frac{H_{DF} - H_{ctrl}}{H_{PF}} \times 100\%, \quad (7)$$

373 where  $H_{DF}$  represents the total hydropower production (for the period 1958–2000) ob-  
 374 tained using realistic forecast-informed operations.  $I_{DF}$  is then combined with  $I_{PF}$  to  
 375 calculate the performance metric  $I$  that quantifies the potential improvement between  
 376 realistic and perfect forecast-informed operations:

$$I = \frac{H_{DF} - H_{ctrl}}{H_{PF} - H_{ctrl}} = \frac{I_{DF}}{I_{PF}}. \quad (8)$$

377 A value of  $I$  equal to 1 indicates that benefits from the actual forecasts equal those uti-  
 378 lizing perfect forecasts. A value of 0 denotes performance equivalent to applying the con-  
 379 trol rules only, while a negative value implies that the forecast-informed scheme is in-  
 380 ferior to the control rules only approach. We calculate this metric only for the subset  
 381 of dams achieving a value of  $I_{PF}$  greater than the mean value of  $I_{PF}$  to better under-  
 382 stand if the benefits modeled with perfect forecasts may be attainable with realistic fore-  
 383 casts.

384 To explain how the metric  $I$  varies, we use a linear regression model accounting for  
 385 both forecast skill and reservoir characteristics. The predictor characterizing the fore-  
 386 cast skill is  $x_{MdAPE}$ , the median absolute percentage error of the forecast, used in place  
 387 of  $KGE$  because it shows a higher correlation with  $I$ . (While  $KGE$  gives a broad view  
 388 of the forecast skill by comparing correlation, mean, and standard deviation of the pre-  
 389 dicted and observed inflows,  $MdAPE$  looks at the forecast error at every time step of  
 390 the inflow time series. This may make  $MdAPE$  a more suitable predictor, since the er-  
 391 ror at each time step affects the release decisions and, ultimately, the hydropower pro-  
 392 duction.) The second predictor is  $x_{exceed}$ , the fraction of time that inflow exceeds the  
 393 maximum turbine release rate. For more details on the choice of predictors, please re-  
 394 fer to Text S3 and Table S3–S4.

395 **4 Results**

396 In this section, we first present the accuracy of the inflow prediction models (Sec-  
 397 tion 4.1) and performance of the forecast-informed schemes (Section 4.2). Then, we quan-

398     tify the extent to which reservoir design characteristics and forecast skill affect the value  
399     of seasonal forecasts (Section 4.3). Lastly, we classify all dams according to their poten-  
400     tial to benefit from forecasts, and identify key geographical regions that may benefit the  
401     most from forecasts (Section 4.4).

#### 402           **4.1 Potential predictors and accuracy**

403           Reservoir inflow exhibits significant correlation with climate and local drivers (po-  
404     tential predictors) at various monthly lags, and these relationships change across the an-  
405     nual cycle. This has a direct influence on expected predictive skill at each hydropower  
406     facility. From a global perspective for monthly dam inflow, the percentage of dams cor-  
407     related with climate and local drivers in each calendar month varies notably (Figure 2).  
408     Evaluating months when a higher percentage of dams are significantly correlated with  
409     predictors, some well-known climatic teleconnections can be observed—for example, ENSO  
410     and winter-spring streamflow in North America and Europe, NAO and spring-summer  
411     peak flows in the northern extratropic regions, and PDO and summer streamflow in south-  
412     eastern North America and central South America (Lee et al., 2018) (see Figure S1). On  
413     average, 27%, 37%, 28%, 20%, and 36% of dams are significantly correlated with ENSO,  
414     NAO, PDO, AMO, and snowfall, respectively. Additionally, and not surprisingly, inflow  
415     for most dams (72%) exhibits significant 1-month lead autocorrelation. An exception is  
416     for some dams during the period March-April, especially in areas with minimal base flow,  
417     such as East Asia (Figures 2 and S1). Soil moisture at a 1-month lead presents corre-  
418     lations at 47% of dams across all months with a seasonality similar to the one expressed  
419     by the inflow.

420           Similar to the results of Lee et al. (2018), reservoir inflow and climate predictors  
421     are often significantly correlated across several lead months. In these cases, climate pre-  
422     dictors are very likely to be included in numerous MP models for various leads, although  
423     the correlations may decrease with longer lead-time. When a climate predictor is signif-  
424     icantly correlated with reservoir inflow at a 1-month lag (MP1), 74% and 38% of the time  
425     that is also included at the 4-month lag (MP4) and 7-month lag (MP7), respectively. Snow-  
426     fall has a similar retention rate. However, and as expected, autocorrelation in inflow and  
427     soil moisture drop more substantially with longer lead; only 53% (28%) of the time when  
428     lagged inflow (soil moisture) is included as a predictor in MP1 is it also still included in  
429     MP4 (MP7). Globally, an average of 2.7, 1.7, and 0.9 predictors are included in the MP1,  
430     MP4, and MP7 models, respectively. In very few cases, the number of predictors increases  
431     with longer lead-time. For months when no potential predictors are identified, or either  
432     MSESS or GSS is less than zero, the long-term mean inflow for that month is used.

433 On average, predictors are identified for 8.3 months (MP1), 6 months (MP4), and  
 434 4.2 months (MP7) (see Figure 3). As noted previously, a lack of long-lead inflow auto-  
 435 correlation is predominantly responsible for this drop-off. Prediction accuracy also de-  
 436 creases with lead-time; average  $KGE$  values are 0.64 and 0.56 for MP1 and MP7, respec-  
 437 tively (Figure 3). Given that prediction accuracy generally declines with lead time, the  
 438 highest  $KGE$  scores across all MP models are associated with MP1 for 68% of dams.  
 439 For the remaining models, the highest prediction accuracy is recorded for 5% (2%) of  
 440 dams in the MP4 (MP7) models, emphasizing that skillful climate teleconnections at longer  
 441 leads do exist, such as in Europe or northwestern and southeastern U.S. (Figure 3b). Glob-  
 442 ally averaged, each MP model illustrates a significant relationship with  $KGE$  scores ( $r$   
 443 = 0.82–0.96 for all MP models). As for the geographical distribution of  $KGE$ , we find  
 444 relatively high  $KGE$  scores in several regions, including North America, eastern South  
 445 America, Europe, and some regions in western Africa and Asia, where inflows correlate  
 446 with most of the predictors considered (Figures 3 and S1).

447 For all MP models, the  $KGE$  has an average value of about 0.56, which is regarded  
 448 as fair skill score. While uniquely tailored forecasts could be produced for each dam con-  
 449 sidering more local influences, the current prediction approach performs well globally and  
 450 reflects achievable long-range inflow prediction. Considering the superior performance  
 451 of the MP1 model, the forecast skill of MP1 only is retained to represent the overall fore-  
 452 cast skill for further analyses.

## 453 4.2 Performance of forecast-informed operations

454 The expected performance of perfect and realistic forecast-informed operations is  
 455 notably different across the 735 hydropower dams (Figure 4). For perfect forecast-informed  
 456 operations (Figure 4a), substantial increases in hydropower production are possible as  
 457 compared with the baseline control rules, represented as expected increase in the per-  
 458 formance metric  $I_{PF}$ . Specifically, 94% of dams exhibit a positive value of  $I_{PF}$ ; mean  
 459 improvement is 4.7% and maximum improvement is 60%. For the small number of dams  
 460 that do not benefit from perfect forecasts, the value of  $I_{PF}$  does not drop below -1.7%.  
 461 Considering all dams collectively, an additional 24 TWh per year of hydroelectricity are  
 462 generated when adopting the perfect forecast-informed approach in lieu of baseline con-  
 463 trol rules (IHA, 2019).

464 When realistic forecast-informed operations are adopted (Figure 4b), a smaller num-  
 465 ber of dams exhibits increased hydropower production; 25% of dams have a positive value  
 466 of  $I_{DF}$ . These 184 dams show an average improvement of 2.3% and can collectively con-  
 467 tribute an additional 1.7 TWh per year in hydropower production. Across all dams, the

468 maximum and minimum values of  $I_{DF}$  are 28% and -24%. This decline in performance,  
 469 as compared with perfect forecasts, is expected, as realistic forecasts introduce a non-  
 470 negligible prediction error. Yet, it should also be noted that less than 20% of dams have  
 471  $KGE$  below 0.5, whereas a disproportionately high number of dams exhibit a negative  
 472  $I_{DF}$  value—a point on which we shall return in Section 4.4. This suggests that for a large  
 473 number of dams control rule-based operations are superior to realistic forecast-informed  
 474 operations. For dams with poor  $I_{DF}$  and high  $KGE$ , the results indicate two points:  $KGE$   
 475 may not fully capture the relationship between forecast skill and value; and reservoir char-  
 476 acteristics may be an important factor influencing the value of realistic forecasts.

### 477 **4.3 Coincident evaluation of prediction accuracy and reservoir charac-** 478 **teristics**

479 To identify the extent to which reservoir characteristics may modulate the value  
 480 of seasonal forecasts, we identify a logistic regression model that explains the likelihood  
 481 of achieving success with perfect forecasts (i.e.,  $I_{PF}$  larger than 4.7%, the mean value  
 482 of  $I_{PF}$  across all dams) as a function of two predictors,  $x_{fill}$  (the ratio of reservoir stor-  
 483 age capacity to the mean monthly inflow) and  $x_{depth}$  (the ratio of maximum reservoir  
 484 depth to maximum hydraulic head). A 10-fold cross-validation yields a model accuracy  
 485 and Kappa statistic of 0.785 and 0.535. (Note that the percentage of dams falling into  
 486 the *success* and *failure* categories is equal to 37% and 63%.)

487 As illustrated in Figure 5 and Table 1, both predictors influence the probability of  
 488 achieving success. For  $x_{fill}$  values exceeding ten months, dams are highly unlikely to ben-  
 489 efit substantially from seasonal forecasts. This suggests that a large storage capacity ef-  
 490 fectively acts as a buffer against inflow uncertainty. Hence, both control rules and per-  
 491 fect forecast-informed operations tend to attain similar performance. We also observe  
 492 that some of the smaller dams ( $x_{fill} < 2$ ) fail to attain increased hydropower production  
 493 even though they are predicted to do so (red triangles in the blue shaded region). This  
 494 may be attributed to the weekly operations, suggesting that more frequent release de-  
 495 cisions may reduce forecast value. For the smaller dams,  $x_{depth}$  becomes a critical fac-  
 496 tor. High values of  $x_{depth}$  indicate that the hydraulic head is highly dependent on the  
 497 reservoir depth, which is in turn dependent on current and near future inflows for dams  
 498 that cannot accumulate large inflow volumes. Thus, forecast-informed operations become  
 499 crucial to maintain a high hydraulic head and maximize hydropower production. For hy-  
 500 dropower dams that have a low value of  $x_{depth}$ , a high hydraulic head is maintained even  
 501 when storage is low, thereby minimizing the utility of forecasts. These are systems re-  
 502 lying on waterfalls, or hilly terrains, to divert part of the water and gain hydraulic head.

503           Considering only the subset of 269 dams that have an  $I_{PF}$  value larger than 4.7%,  
 504 we apply a linear regression model to estimate the performance metric  $I$ . This time, the  
 505 predictors include  $x_{MdAPE}$  (median absolute percentage error of forecast inflows) and  
 506  $x_{exceed}$  (the fraction of time that inflow exceeds the maximum turbine release rate). The  
 507 linear regression model has an adjusted  $R^2$  of 0.31—a reasonable performance if we con-  
 508 sider that the relationship between forecast skill, value, and reservoir characteristics is  
 509 explained using two predictors. The reader is referred to Table S3-4 for more complex  
 510 models that include additional predictors.

511           The results are presented in Table 2 and illustrated in Figure 6. As expected, higher  
 512 forecast skill (lower  $x_{MdAPE}$ ) increases the potential benefits realized by the realistic fore-  
 513 casts; a 1% decrease in  $x_{MdAPE}$  increases  $I$  by 0.03. Reservoir characteristics can play  
 514 an important role, as certain configurations allow dams and hydropower production to  
 515 benefit from realistic forecasts. Specifically, we find that dams that have large fractions  
 516 of time in which inflow exceeds the maximum turbine release (large values of  $x_{exceed}$ )  
 517 are expected to benefit from forecast-informed operations—even when forecasts are not  
 518 very accurate (as shown by the diagonal divide in Figure 6). This is predominantly a re-  
 519 sult of both forecast and observed inflow exceeding the maximum turbine release rate  
 520 at many time steps, a situation in which the release decision would be the same regardless—  
 521 inaccurate forecast will not penalize hydropower production.

#### 522           **4.4 A classification of hydropower dams**

523           Banking on the results described above, we divide the dams into four categories  
 524 on the basis of their potential to benefit from perfect forecast-informed operations (*high*  
 525 *potential* if  $I_{PF} > 4.7\%$  and *low potential* otherwise) and forecast skill (*good forecast*  
 526 if  $x_{MdAPE} < 20\%$  and *poor forecast* otherwise). The cut-off value for  $I_{PF}$  is inherited  
 527 from the previous analysis (logistic regression model), while the cut-off for  $x_{MdAPE}$  di-  
 528 vides the 735 dams into two groups containing one third (*good forecast*) and two thirds  
 529 (*poor forecast*) of the observations. Two groups of dams of particular interest includes  
 530 (1) dams that fall in regions expressing strong forecast accuracy and have the potential  
 531 to reap benefits from forecast-informed operations (9% of the total number of reservoirs),  
 532 and (2) dams with strong potential to benefit from forecast-informed operations but lack  
 533 forecast accuracy (27%) (Table 3).

534           As show in Section 4.3, the potential of a dam to benefit from forecasts is largely  
 535 dependant on its design specifications, which present comparable values in areas with  
 536 similar orography and design practices. Forecast skill, on the other hand, is largely de-  
 537 pendant on climate and teleconnections, which tend to present regional patterns. With

538 this information at hand, we illustrate in Figure 7 the distribution of the four groups of  
 539 dams across the thirty climate zones of the Köppen-Geiger climate classification system.  
 540 Statistics for each climate zone, together with their significance calculated using Chi-squared  
 541 test, are listed in Table 3. We notice a few interesting regions. First, hydropower dams  
 542 in Central Europe have neither accurate forecast nor high potential to benefit from forecast-  
 543 informed operations. This trend is significant ( $p < 0.05$ ) for dams in the Alps (alpine  
 544 climate, *ET*), in particular for dams that have large capacity-inflow ratios and high hy-  
 545 draulic heads. Second, hydropower dams in the tropical savanna climate (*Aw*, Thailand,  
 546 India, Brazil, and western Africa) and subarctic climate (*Dfc*, Canada, Russia, eastern  
 547 Europe) have accurate forecast but poor to fair potential. Good forecast skill in the trop-  
 548 ical savanna (subarctic) climate can be attributed to the high correlation with lagged stream-  
 549 flow, ENSO, PDO, and AMO (snowfall, PDO, and NAO) teleconnections (Figure S1).  
 550 Third, dams in many regions have high potential to benefit but lack accurate forecast.  
 551 This is particularly pronounced in the humid subtropical climate (*Cwa*, *Cfa*) lying in  
 552 the southeast regions of Australia, China, U.S., and South America. The trend is also  
 553 true—but not significant—for dams in Southeast Asia (tropical rainforest, *Af*) and Pa-  
 554 cific Northwest in the U.S. (warm summer Mediterranean, *Csb*).

## 555 5 Discussion

### 556 5.1 Implications for planning and management of hydropower projects

557 In this study, we examine the relationship between seasonal streamflow forecasts  
 558 and global hydropower production, accounting for the influence of reservoir character-  
 559 istics. Specifically, we develop seasonal inflow forecasts for 735 headwater dams based  
 560 on lagged global and local hydro-climatic variables. The forecasts exhibit modest skill  
 561 globally, but higher skill in several regions, including the snow-dominated northern ex-  
 562 tratropic region and the tropical savannah climate in mainland Southeast Asia, eastern  
 563 South America, and western Africa. In agreement with earlier works, our forecasts ex-  
 564 hibit well-known teleconnections, such as the one between NAO and spring summer peak  
 565 flow in northern extratropic regions (Lee et al., 2018) or the one between ENSO and stream-  
 566 flow in Southeast Asia (Sankarasubramanian et al., 2009; Räsänen & Kummu, 2013) and  
 567 winter-spring streamflow in the Pacific Northwest (Hamlet et al., 2002; Voisin et al., 2006).

568 We then seek to uncover the relationship between forecast skill, value, and reser-  
 569 voir characteristics by adopting forecasts in the reservoir operations model. While 94%  
 570 of the dams could benefit from perfect forecasts, only 25% demonstrate improvements  
 571 when using our realistic forecasts—a fairly low percentage if we consider the forecast skill  
 572 achieved globally. This highlights the fundamental role of reservoir characteristics in shap-

573 ing the relationship between forecast skill and value. Key design specifications include  
574 a short time-to-fill—a characteristic identified by a few recent studies (Anghileri et al.,  
575 2016; Turner, Bennett, et al., 2017; Yang et al., 2020)—an hydraulic head largely depen-  
576 dent on reservoir depth, and inflows often exceeding the maximum turbine release, a de-  
577 sign specification that allows operators to work with a larger margin of forecast error dur-  
578 ing high inflow periods. It is worth stressing here that these results are not intended to  
579 provide site operation guidelines, but do represent a first, qualitative, step towards de-  
580 termining the potential benefit of seasonal streamflow forecasts for hydropower opera-  
581 tors. The relationships identified here could for example be used to understand how much  
582 skill is required for the reservoir inflow forecasts or to characterize the interplay between  
583 climatology, hydrology, and dam characteristics in a large region of interest.

584 By combining information on reservoir characteristics, forecast skill, and climatic  
585 zones, we finally identify large regions in which dams would benefit the most from fore-  
586 casts. A particularly interesting group is formed by dams with strong potential to ben-  
587 efit from forecast-informed operations but lacking adequate forecast accuracy—located  
588 in the maritime Southeast Asia, the Pacific Northwest and the humid subtropical climate  
589 of the southeast regions of Australia, China, U.S., and South America. These are areas  
590 in which watershed-specific analysis may bring immediate benefits to hydropower op-  
591 erators. It is also worth mentioning that the implications of our study go beyond exist-  
592 ing reservoirs; dam planning over large scales may also benefit of some of our findings.  
593 For example, one could evaluate information on untapped hydropower potential (Y. Zhou  
594 et al., 2015; Hoes et al., 2017) and seasonal streamflow predictability to derive some first,  
595 qualitative, conclusions on the expected reservoir characteristics. A case in point are run-  
596 of-the-river dams: these systems present short time-to-fill and are therefore suitable to  
597 implement forecast-informed reservoir sizing and operations (Bertoni et al., 2020).

## 598 **5.2 Limitations and opportunities**

599 Given the global nature of this study, it is important to note that these results and  
600 their implications are not meant to provide site-specific guidelines, but rather qualita-  
601 tive information for watershed-specific studies. Like any other global study, the large spa-  
602 tial domain requires building on a number of assumptions that must be discussed to put  
603 our results into perspective.

604 First, we assume that the goal of dam operators is to maximize hydropower pro-  
605 duction over the long term (in addition to providing flood control). While this objec-  
606 tive provides a tangible indication of forecast value, it may not be fully representative  
607 of the local conditions encountered by operators. For example, operators may be inter-

608 ested to maximize revenue (Anghileri et al., 2018) supply the bulk of power to the grid  
 609 (Zambon et al., 2012), or complement the generation of other renewable (Graabak et al.,  
 610 2019). To account explicitly for these aspects, one needs to model the role that dams play  
 611 in the power market, as recently done for the Western U.S. (Voisin et al., 2020), Eng-  
 612 land (Byers et al., 2020), Laos (A. K. Chowdhury et al., 2020), and the Greater Mekong  
 613 (K. A. Chowdhury et al., 2020). With these models, one could also infer the willingness  
 614 to pay for improved streamflow forecasts.

615 Second, release decisions at individual dams may be affected by joint operations  
 616 between multiple reservoirs and supported with more accurate data and tailor-made hy-  
 617 drological models than those adopted here. Importantly, these data could include qual-  
 618 itative or quantitative forecasts. Although precipitation and streamflow predictions are  
 619 not used consistently across the world (Adams & Pagano, 2016), one must acknowledge  
 620 that medium- to long-range forecasts are increasingly adopted by water utilities—as re-  
 621 cently shown by Turner et al. (2020) for 300 dams in the conterminous United States.  
 622 Access to observed and inferred release decisions could thus help researchers provide a  
 623 more robust and nuanced estimate of forecast value.

## 624 **6 Conclusions**

625 Our study suggests that skilful forecasts generally lead to increasing benefits, with  
 626 such benefits strongly modulated by reservoirs characteristics. However, for some dams,  
 627 even accurate forecasts may not improve hydropower production if reservoir character-  
 628 istics are not suitable. On the flipside, some dams can be profitable with little regard  
 629 to forecast accuracy if their design specifications meet such conditions. Research that  
 630 integrates these findings with hydrological-electricity models to quantify economic ben-  
 631 efits is warranted. Specifically, this may reflect the willingness to pay for improved fore-  
 632 cast models. Such an assessment could provide guidance and insights for large-scale hy-  
 633 dropower planning and management, particularly as energy systems become more in-  
 634 terconnected.

## 635 **Appendix A Skill scores for model validation**

636 The mean squared error skill score (MSESS) is a deterministic skill score that com-  
 637 pares the MSE of prediction model and climatology. It is defined as follows (Wilks, 2011):

$$MSESS = \left( 1 - \frac{MSE_{pred}}{MSE_{clim}} \right), \quad (A1)$$

638 where  $MSE_{pred}$  is the MSE of prediction, and  $MSE_{clim}$  is the MSE of climatological  
 639 mean prediction. The perfect score of the MESS is 1, while a value equal to 0 indicates  
 640 that the model skill is equal to that of the climatology.

641 The Gerrity skill score (GSS) is a multi-categorical skill score that rewards correct  
 642 predictions in rarer categories. The GSS is calculated as follows:

$$GSS = \sum_{i=1}^3 \sum_{j=1}^3 p_{ij} s_{ij}, \quad (\text{A2})$$

643 where  $p_{ij}$  is the joint probability of inflow in each category ( $i, j$ ) of a contingency table  
 644 (3 x 3 in this study) and  $s_{ij}$  is a scoring weight to yield more or less credits based on the  
 645 frequency of the category (Wilks, 2011). The three categories correspond to the upper,  
 646 middle, and lower thirds of the inflow during the model calibration period. The GSS ranges  
 647 from -1 to 1, where a value of 1 represents a perfect forecast and a value of 0 means no  
 648 predictive skill (compared to the climatology).

## 649 **Acknowledgments**

650 Jia Yi Ng and Stefano Galelli are supported by Singapore's Ministry of Education (MoE)  
 651 through the Tier 2 project 'Linking water availability to hydropower supply—an engi-  
 652 neering systems approach' (Award No. MOE2017-T2-1-143). All simulations results are  
 653 available on HydroShare at <http://www.hydroshare.org/resource/ca365ffb1a1f49df8b77e393be965fd8>.  
 654 We thank the Associate Editor and three anonymous reviewers for their constructive com-  
 655 ments.

## 656 **References**

- 657 Adams, T. E., & Pagano, T. C. (2016). *Flood forecasting: A global perspective*. Aca-  
 658 demic Press.
- 659 Ahmad, S. K., & Hossain, F. (2019). A generic data-driven technique for forecast-  
 660 ing of reservoir inflow: Application for hydropower maximization. *Environmental*  
 661 *Modelling & Software*, *119*, 147–165.
- 662 Alcamo, J., Döll, P., Henrichs, T., Kaspar, F., Lehner, B., Rösch, T., & Siebert, S.  
 663 (2003). Development and testing of the WaterGAP 2 global model of water use  
 664 and availability. *Hydrological Sciences Journal*, *48*(3), 317–337.
- 665 Anghileri, D., Castelletti, A., & Burlando, P. (2018). Alpine hydropower in the  
 666 decline of the nuclear era: Trade-off between revenue and production in the  
 667 Swiss Alps. *Journal of Water Resources Planning and Management*, *144*(8),  
 668 04018037.

- 669 Anghileri, D., Monhart, S., Zhou, C., Bogner, K., Castelletti, A., Burlando, P., &  
670 Zappa, M. (2019). The value of subseasonal hydrometeorological forecasts  
671 to hydropower operations: how much does pre-processing matter? *Water*  
672 *Resources Research*, *55*, 10159–10178.
- 673 Anghileri, D., Voisin, N., Castelletti, A., Pianosi, F., Nijssen, B., & Lettenmaier,  
674 D. P. (2016). Value of long-term streamflow forecasts to reservoir opera-  
675 tions for water supply in snow-dominated river catchments. *Water Resources*  
676 *Research*, *52*(6), 4209–4225.
- 677 Bertoni, F., Castelletti, A., Giuliani, M., & Read, P. M. (2020). Designing with in-  
678 formation feedbacks: Forecast informed reservoir sizing and operation. *Earth*  
679 *and Space Science Open Archive ESSOAr*.
- 680 Bertsekas, D. (1976). *Dynamic programming and stochastic control*. New York, New  
681 York: Academic Press.
- 682 Block, P. (2011). Tailoring seasonal climate forecasts for hydropower operations. *Hy-*  
683 *drology and Earth System Sciences*, *15*(4), 1355–1368.
- 684 Bonnema, M., & Hossain, F. (2017). Inferring reservoir operating patterns across  
685 the Mekong Basin using only space observations. *Water Resources Research*,  
686 *53*(5), 3791–3810.
- 687 Busker, T., de Roo, A., Gelati, E., Schwatke, C., Adamovic, M., Bisselink, B., . . .  
688 Cottam, A. (2019). A global lake and reservoir volume analysis using a surface  
689 water dataset and satellite altimetry. *Hydrology and Earth System Sciences*,  
690 *23*(2), 669–690.
- 691 Byers, E. A., Coxon, G., Freer, J., & Hall, J. W. (2020). Drought and climate  
692 change impacts on cooling water shortages and electricity prices in Great  
693 Britain. *Nature Communications*, *11*(1), 1–12.
- 694 Chowdhury, A. K., Dang, T. D., Bagchi, A., & Galelli, S. (2020). Expected bene-  
695 fits of Laos’ hydropower development curbed by hydroclimatic variability and  
696 limited transmission capacity: Opportunities to reform. *Journal of Water*  
697 *Resources Planning and Management*, *146*(10), 05020019.
- 698 Chowdhury, K. A., Dang, T. D., Nguyen, H. T., Koh, R., & Galelli, S. (2020). The  
699 Greater Mekong’s climate-water-energy nexus: how ENSO-triggered regional  
700 droughts affect power supply and CO<sub>2</sub> emissions. *Earth and Space Science*  
701 *Open Archive ESSOAr*.
- 702 De Felice, M., Dubus, L., Suckling, E., & Troccoli, A. (2018, Jul). *The impact of the*  
703 *North Atlantic Oscillation on European hydro-power generation*. EarthArXiv.  
704 Retrieved from [eartharxiv.org/8sntx](https://eartharxiv.org/8sntx) doi: 10.31223/osf.io/8sntx
- 705 Döll, P., Fiedler, K., & Zhang, J. (2009). Global-scale analysis of river flow alter-

- 706 ations due to water withdrawals and reservoirs. *Hydrology and Earth System*  
707 *Sciences*, 13(12), 2413–2432.
- 708 Döll, P., & Lehner, B. (2002). Validation of a new global 30-min drainage direction  
709 map. *Journal of Hydrology*, 258(1-4), 214–231.
- 710 Enfield, D. B., Mestas-Nuñez, A. M., & Trimble, P. J. (2001). The Atlantic mul-  
711 tidecadal oscillation and its relation to rainfall and river flows in the conti-  
712 nental US. *Geophysical Research Letters*, 28(10), 2077–2080. Retrieved from  
713 <https://doi.org/10.1029/2000GL012745>
- 714 Gao, H., Birkett, C., & Lettenmaier, D. P. (2012). Global monitoring of large reser-  
715 voir storage from satellite remote sensing. *Water Resources Research*, 48(9).
- 716 Gelati, E., Madsen, H., & Rosbjerg, D. (2014). Reservoir operation using El Niño  
717 forecasts—case study of Daule Peripa and Baba, Ecuador. *Hydrological Sci-*  
718 *ences Journal*, 59(8), 1559–1581.
- 719 GEO. (2016). *Global Energy Observatory: Information on Global Energy Systems*  
720 *and Infrastructure*. (Available online at <http://globalenergyobservatory.org>)
- 721 Graabak, I., Korpås, M., Jaehnert, S., & Belsnes, M. (2019). Balancing future vari-  
722 able wind and solar power production in Central-West Europe with Norwegian  
723 hydropower. *Energy*, 168, 870–882.
- 724 Grill, G., Lehner, B., Thieme, M., Geenen, B., Tickner, D., Antonelli, F., . . . oth-  
725 ers (2019). Mapping the world’s free-flowing rivers. *Nature*, 569(7755), 215.  
726 Retrieved from <http://www.nature.com/articles/s41586-019-1111-9>
- 727 Gupta, H. V., Kling, H., Yilmaz, K. K., & Martinez, G. F. (2009). Decomposition  
728 of the mean squared error and NSE performance criteria: Implications for  
729 improving hydrological modelling. *Journal of hydrology*, 377(1-2), 80–91.
- 730 Haddeland, I., Heinke, J., Biemans, H., Eisner, S., Flörke, M., Hanasaki, N., . . . oth-  
731 ers (2014). Global water resources affected by human interventions and climate  
732 change. *Proceedings of the National Academy of Sciences*, 111(9), 3251–3256.
- 733 Hamlet, A. F., Huppert, D., & Lettenmaier, D. P. (2002). Economic value of long-  
734 lead streamflow forecasts for Columbia River hydropower. *Journal of Water*  
735 *Resources Planning and Management*, 128(2), 91–101.
- 736 Hamududu, B., & Killingtveit, A. (2012). Assessing climate change impacts on  
737 global hydropower. *Energies*, 5(2), 305–322.
- 738 Hejazi, M. I., Cai, X., & Ruddell, B. L. (2008). The role of hydrologic information  
739 in reservoir operation—learning from historical releases. *Advances in Water Re-*  
740 *sources*, 31(12), 1636–1650.
- 741 Hoes, O. A., Meijer, L. J., Van Der Ent, R. J., & Van De Giesen, N. C. (2017). Sys-  
742 tematic high-resolution assessment of global hydropower potential. *PloS one*,

- 743           12(2), e0171844.
- 744 Hurrell, J. W., & Deser, C. (2010). North Atlantic climate variability: the role of the  
745 North Atlantic Oscillation. *Journal of Marine Systems*, 79(3-4), 231–244. Re-  
746 trieved from <https://doi.org/10.1016/j.jmarsys.2009.11.002>
- 747 ICOLD. (2011). *World Register of Dams. Version Updates 1998–2009* (Tech. Rep.).  
748 Paris, France: International Commission on Large Dams. (Available online at  
749 [www.icold-cigb.net](http://www.icold-cigb.net))
- 750 IHA. (2019). *2019 hydropower status report* (Tech. Rep.). Retrieved from [https://](https://www.hydropower.org/status2019)  
751 [www.hydropower.org/status2019](https://www.hydropower.org/status2019)
- 752 Jolliffe, I. (2002). *Principal component analysis*. Cambridge MA: Springer-Verlag  
753 New York. doi: 10.1007/b98835
- 754 Kao, S.-C., Sale, M. J., Ashfaq, M., Martinez, R. U., Kaiser, D. P., Wei, Y., & Dif-  
755 fenbaugh, N. S. (2015). Projecting changes in annual hydropower generation  
756 using regional runoff data: An assessment of the United States federal hy-  
757 dropower plants. *Energy*, 80, 239–250.
- 758 Kaveh, K., Hosseinjanzadeh, H., & Hosseini, K. (2013). A new equation for calcu-  
759 lation of reservoir’s area-capacity curves. *KSCE Journal of Civil Engineering*,  
760 17(5), 1149–1156.
- 761 Kim, Y.-O., & Palmer, R. N. (1997). Value of seasonal flow forecasts in Bayesian  
762 stochastic programming. *Journal of Water Resources Planning and Manage-*  
763 *ment*, 123(6), 327–335.
- 764 Lee, D., Ward, P., & Block, P. (2018). Attribution of large-scale climate patterns to  
765 seasonal peak-flow and prospects for prediction globally. *Water Resources Re-*  
766 *search*, 54(2), 916–938. doi: 10.1002/2017WR021205
- 767 Lehner, B., Czisch, G., & Vassolo, S. (2005). The impact of global change on the  
768 hydropower potential of Europe: a model-based analysis. *Energy Policy*, 33(7),  
769 839–855.
- 770 Lehner, B., & Döll, P. (2004). Development and validation of a global database of  
771 lakes, reservoirs and wetlands. *Journal of Hydrology*, 296(1), 1–22.
- 772 Lehner, B., Liermann, C. R., Revenga, C., Vörösmarty, C., Fekete, B., Couzet,  
773 P., ... others (2011). High-resolution mapping of the world’s reservoirs and  
774 dams for sustainable river-flow management. *Frontiers in Ecology and the*  
775 *Environment*, 9(9), 494–502.
- 776 Lehner, B., Verdin, K., & Jarvis, A. (2008). New global hydrography derived from  
777 spaceborne elevation data. *Eos, Transactions American Geophysical Union*,  
778 89(10), 93–94.
- 779 Libisch-Lehner, C., Nguyen, H., Taormina, R., Nachtnebel, H., & Galelli, S. (2019).

- 780 On the value of ENSO state for urban water supply system operators: Op-  
781 portunities, trade-offs, and challenges. *Water Resources Research*, 55(4),  
782 2856–2875.
- 783 Liebe, J., Van De Giesen, N., & Andreini, M. (2005). Estimation of small reservoir  
784 storage capacities in a semi-arid environment: A case study in the Upper East  
785 Region of Ghana. *Physics and Chemistry of the Earth, Parts A/B/C*, 30(6),  
786 448–454.
- 787 Liu, X., Tang, Q., Voisin, N., & Cui, H. (2016). Projected impacts of climate change  
788 on hydropower potential in China. *Hydrology and Earth System Sciences*,  
789 20(8), 3343–3359.
- 790 Loucks, D. P., Van Beek, E., Stedinger, J. R., Dijkman, J. P., & Villars, M. T.  
791 (2005). *Water resources systems planning and management: an introduction to*  
792 *methods, models and applications*. Paris: UNESCO.
- 793 Maurer, E. P., & Lettenmaier, D. P. (2004). Potential effects of long-lead hydrologic  
794 predictability on Missouri River main-stem reservoirs. *Journal of Climate*,  
795 17(1), 174–186.
- 796 McHugh, M. L. (2012). Interrater reliability: the kappa statistic. *Biochemia medica:*  
797 *Biochemia medica*, 22(3), 276–282.
- 798 Ng, J. Y., Turner, S. W., & Galelli, S. (2017). Influence of El Niño Southern Oscilla-  
799 tion on global hydropower production. *Environmental Research Letters*, 12(3),  
800 034010.
- 801 Pastor, A., Ludwig, F., Biemans, H., Hoff, H., & Kabat, P. (2014). Accounting for  
802 environmental flow requirements in global water assessments. *Hydrology and*  
803 *Earth System Sciences*, 18(12), 5041–5059.
- 804 Payne, J. T., Wood, A. W., Hamlet, A. F., Palmer, R. N., & Lettenmaier, D. P.  
805 (2004). Mitigating the effects of climate change on the water resources of the  
806 Columbia River basin. *Climatic change*, 62(1-3), 233–256.
- 807 Peel, M. C., Finlayson, B. L., & McMahon, T. A. (2007). Updated world map of the  
808 Köppen-Geiger climate classification. *Hydrology and Earth System Sciences*,  
809 11(5).
- 810 Räsänen, T. A., & Kumm, M. (2013). Spatiotemporal influences of ENSO on pre-  
811 cipitation and flood pulse in the Mekong River Basin. *Journal of Hydrology*,  
812 476, 154–168.
- 813 Rheinheimer, D. E., Bales, R. C., Oroza, C. A., Lund, J. R., & Viers, J. H. (2016).  
814 Valuing year-to-go hydrologic forecast improvements for a peaking hydropower  
815 system in the Sierra Nevada. *Water Resources Research*, 52(5), 3815–3828.
- 816 Sankarasubramanian, A., Lall, U., Devineni, N., & Espinueva, S. (2009). The role of

- 817 monthly updated climate forecasts in improving intraseasonal water allocation.  
 818 *Journal of Applied Meteorology and Climatology*, 48(7), 1464–1482.
- 819 Soncini-Sessa, R., Weber, E., & Castelletti, A. (2007). *Integrated and participatory*  
 820 *water resources management—Theory* (Vol. 1). Amsterdam, NL: Elsevier.
- 821 Turner, S. W., Bennett, J. C., Robertson, D. E., & Galelli, S. (2017). Complex  
 822 relationship between seasonal streamflow forecast skill and value in reservoir  
 823 operations. *Hydrology and Earth System Sciences*, 21(9), 4841–4859.
- 824 Turner, S. W., & Galelli, S. (2016). Water supply sensitivity to climate change: an  
 825 R package for implementing reservoir storage analysis in global and regional  
 826 impact studies. *Environmental Modelling & Software*, 76, 13–19.
- 827 Turner, S. W., Hejazi, M., Kim, S. H., Clarke, L., & Edmonds, J. (2017). Climate  
 828 impacts on hydropower and consequences for global electricity supply invest-  
 829 ment needs. *Energy*, 141, 2081–2090.
- 830 Turner, S. W., Ng, J. Y., & Galelli, S. (2017). Examining global electricity supply  
 831 vulnerability to climate change using a high-fidelity hydropower dam model.  
 832 *Science of the Total Environment*, 590, 663–675.
- 833 Turner, S. W., Xu, W., & Voisin, N. (2020). Inferred inflow forecast horizons guiding  
 834 reservoir release decisions across the united states. *Hydrology and Earth Sys-*  
 835 *tem Sciences*, 24, 1275–1291.
- 836 Van Beek, L., Wada, Y., & Bierkens, M. F. (2011). Global monthly water stress: 1.  
 837 water balance and water availability. *Water Resources Research*, 47(7).
- 838 Van Vliet, M. T., Wiberg, D., Leduc, S., & Riahi, K. (2016). Power-generation  
 839 system vulnerability and adaptation to changes in climate and water resources.  
 840 *Nature Climate Change*, 6(4), 375.
- 841 Voisin, N., Dyreson, A., Fu, T., O’Connell, M., Turner, S. W., Zhou, T., & Mack-  
 842 nick, J. (2020). Impact of climate change on water availability and its propa-  
 843 gation through the Western US power grid. *Applied Energy*, 276, 115467.
- 844 Voisin, N., Hamlet, A. F., Graham, L. P., Pierce, D. W., Barnett, T. P., & Let-  
 845 tenmaier, D. P. (2006). The role of climate forecasts in Western US power  
 846 planning. *Journal of applied meteorology and climatology*, 45(5), 653–673.
- 847 Ward, P. J., Eisner, S., Flörke, M., Dettinger, M. D., & Kummerow, M. (2014). Annual  
 848 flood sensitivities to El Niño–Southern Oscillation at the global scale. *Hydro-*  
 849 *logy and Earth System Sciences*, 18(1), 47–66.
- 850 Weedon, G., Gomes, S., Viterbo, P., Shuttleworth, W. J., Blyth, E., Österle, H., . . .  
 851 Best, M. (2011). Creation of the WATCH forcing data and its use to assess  
 852 global and regional reference crop evaporation over land during the twentieth  
 853 century. *Journal of Hydrometeorology*, 12(5), 823–848.

- 854 Wilks, D. S. (2011). *Statistical methods in the atmospheric sciences* (Vol. 100). Aca-  
855 demic press.
- 856 Yang, G., Guo, S., Liu, P., & Block, P. (2020). Integration and evaluation of  
857 forecast-informed multiobjective reservoir operations. *Journal of Water Re-*  
858 *sources Planning and Management*, *146*(6), 04020038.
- 859 You, J.-Y., & Cai, X. (2008). Determining forecast and decision horizons for reser-  
860 voir operations under hedging policies. *Water resources research*, *44*(11).
- 861 Zambon, R. C., Barros, M. T. L., Lopes, J. E. G., Barbosa, P. S. F., Francato,  
862 A. L., & Yeh, W. W.-G. (2012). Optimization of large-scale hydrothermal  
863 system operation. *Journal of Water Resources Planning and Management*,  
864 *138*(2), 135-143.
- 865 Zarfl, C., Lumsdon, A. E., Berlekamp, J., Tydecks, L., & Tockner, K. (2015). A  
866 global boom in hydropower dam construction. *Aquatic Sciences*, *77*(1), 161–  
867 170.
- 868 Zeng, R., Cai, X., Ringler, C., & Zhu, T. (2017). Hydropower versus irrigation—an  
869 analysis of global patterns. *Environmental Research Letters*, *12*(3), 034006.
- 870 Zhang, X., Li, H.-Y., Deng, Z. D., Ringler, C., Gao, Y., Hejazi, M. I., & Leung,  
871 L. R. (2018). Impacts of climate change, policy and water-energy-food nexus  
872 on hydropower development. *Renewable energy*, *116*, 827–834.
- 873 Zhang, Y., Wallace, J. M., & Battisti, D. S. (1997). ENSO-like interdecadal variabil-  
874 ity: 1900–93. *Journal of climate*, *10*(5), 1004–1020. Retrieved from [https://](https://doi.org/10.1175/1520-0442(1997)010<1004:ELIV>2.0.CO;2)  
875 [doi.org/10.1175/1520-0442\(1997\)010<1004:ELIV>2.0.CO;2](https://doi.org/10.1175/1520-0442(1997)010<1004:ELIV>2.0.CO;2)
- 876 Zhao, T., Yang, D., Cai, X., Zhao, J., & Wang, H. (2012). Identifying effective fore-  
877 cast horizon for real-time reservoir operation under a limited inflow forecast.  
878 *Water Resources Research*, *48*(1).
- 879 Zhou, T., Voisin, N., & Fu, T. (2018). Non-stationary hydropower generation pro-  
880 jections constrained by environmental and electricity grid operations over the  
881 western United States. *Environmental Research Letters*, *13*(7), 074035.
- 882 Zhou, Y., Hejazi, M., Smith, S., Edmonds, J., Li, H., Clarke, L., . . . Thomson, A.  
883 (2015). A comprehensive view of global potential for hydro-generated electric-  
884 ity. *Energy & Environmental Science*, *8*(9), 2622–2633.

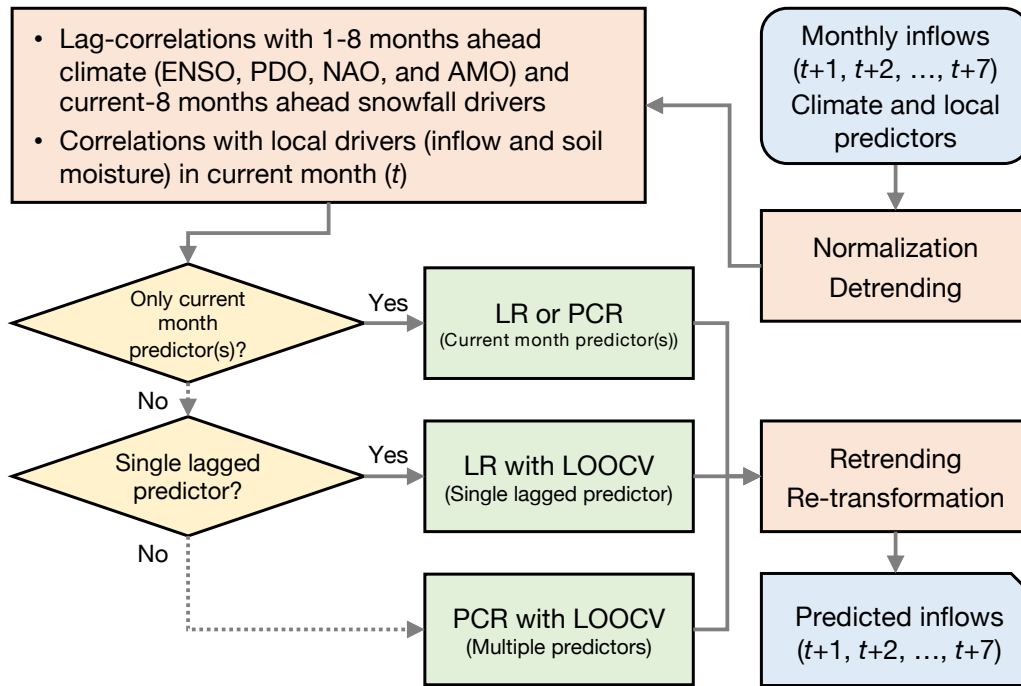


**Figure 1.** Graphical representation of the monthly prediction (MP) model scheme. At each calendar month  $t$ , we develop seven independent models to predict monthly inflows for the next seven months: MP1 ( $t + 1$ ), MP2 ( $t + 2$ ), ..., MP7 ( $t + 7$ ).

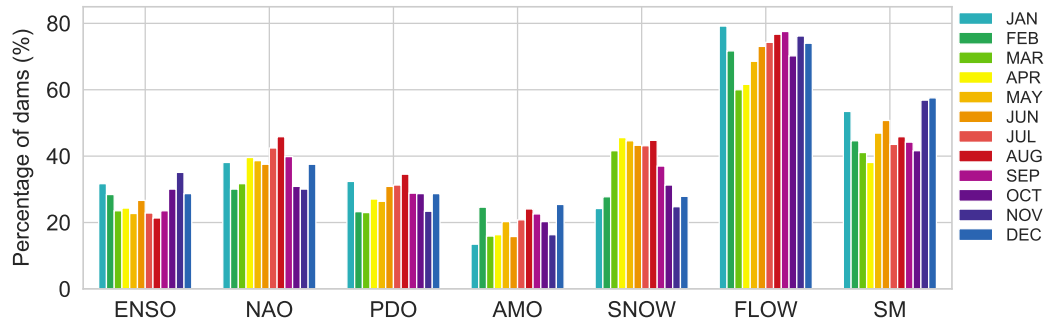


**Figure 2.** Percentage of dams significantly correlated with lagged predictors (ENSO, NAO, PDO, AMO, and snowfall) and 1-month ahead predictors (inflow and soil moisture) in each calendar month.

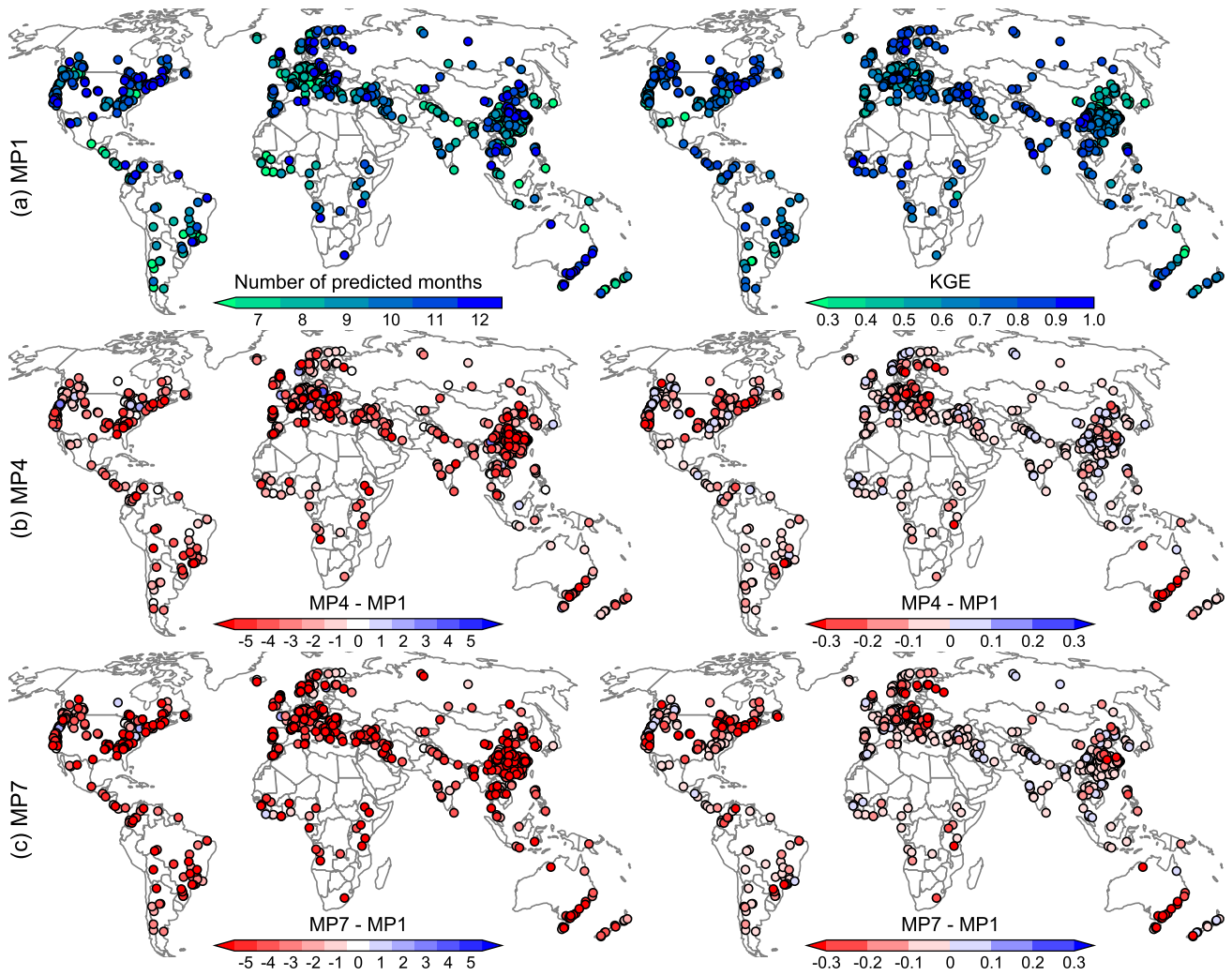


**Figure 3.** Number of predicted months (left) and *KGE* (right) of MP1 (a) and differences with respect to MP4 (b) and MP7 (c).

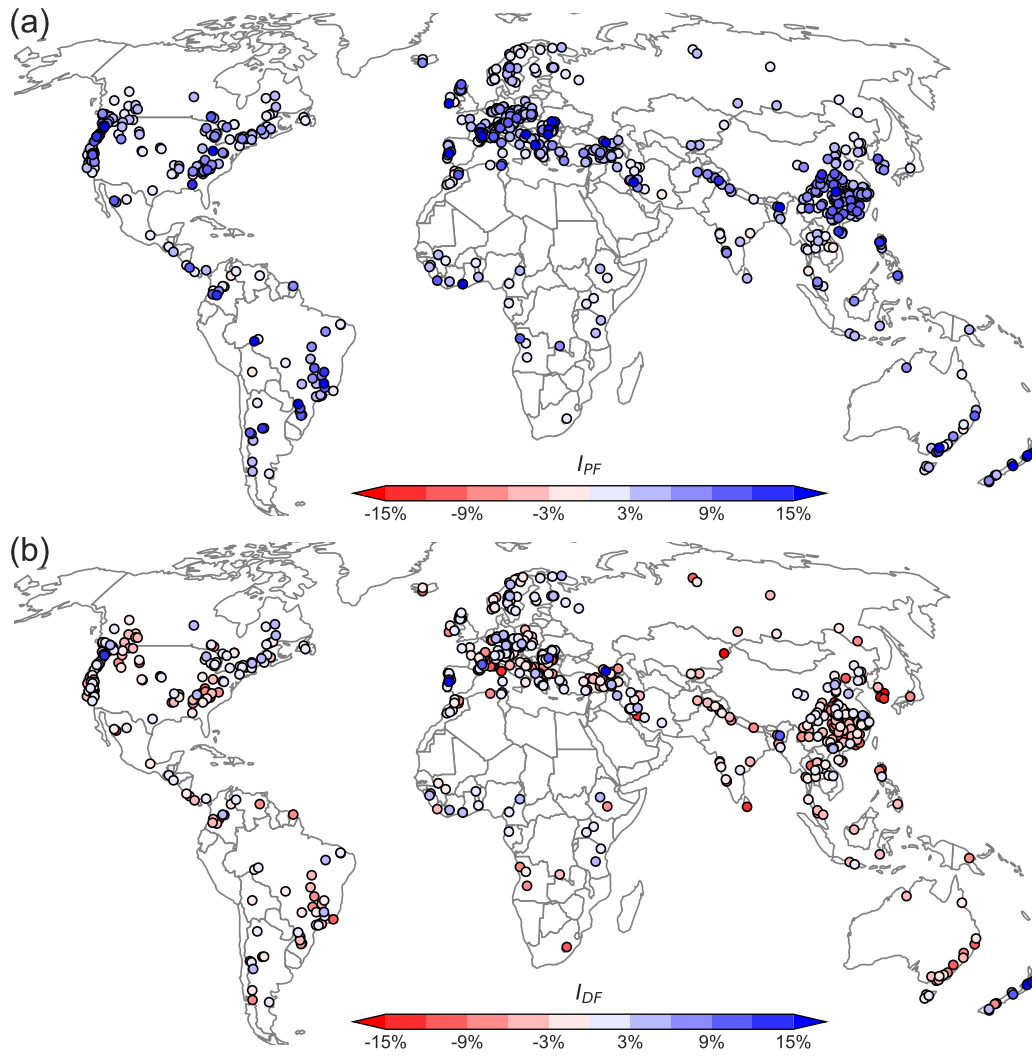


**Figure 4.** Improvements in hydropower production using perfect (a) and realistic (b) forecasts. The terms  $I_{PF}$  and  $I_{DF}$  indicate the relative improvement in hydropower production (with respect to the basic control rules) provided by perfect and realistic forecasts. Nearly all dams are able to benefit from perfect forecasts, but only 25% of dams benefits from realistic forecasts.

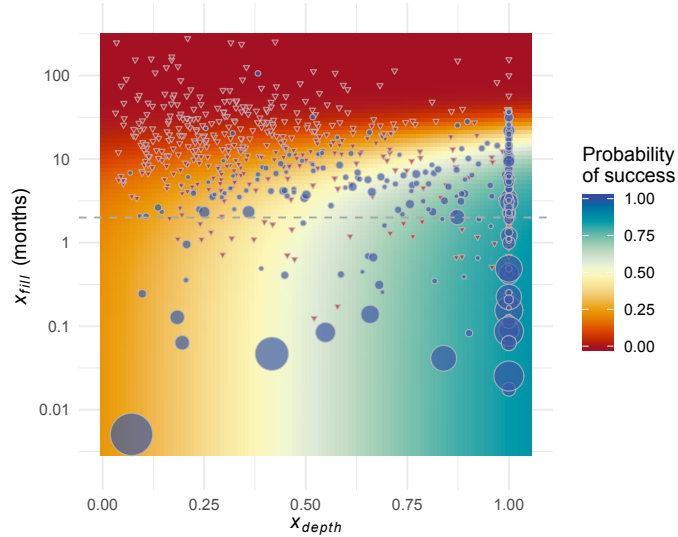


**Figure 5.** Probability of *success* estimated using a logistic regression model with predictors  $x_{depth}$  and  $x_{fill}$  (in log scale). Red corresponds to a probability of success equal to zero, meaning that the dam is likely to do well with the control rules. Blue represents a probability of success equal to 1, meaning that a dam is likely to benefit from forecast-informed operations. Each point in the plot represents one of the 735 dams. Blue circles represent dams labelled as *success* ( $I_{PF} > 4.7\%$ ) and red triangles represents *failures*. The size of the blue circles represents the value of  $I_{PF}$ . All red triangles have the same size. Dams below the dashed line ( $x_{fill} = 2$ ) are operated with a weekly time step. Dams with low values of  $x_{fill}$  (small storage capacity relative to inflow rate) and high  $x_{depth}$  (lacking a natural waterfall) are more likely to benefit from forecast-informed operations.

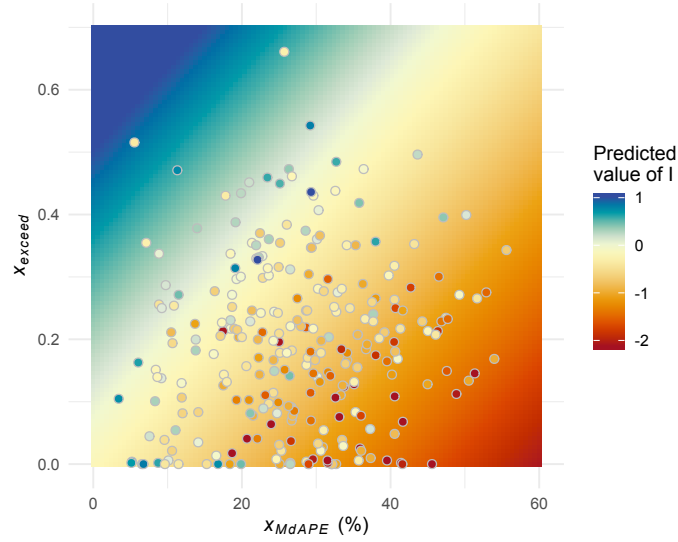


**Figure 6.** Potential benefits realized by realistic forecast ( $I$ ) predicted using linear regression with predictors  $x_{exceed}$  and the median absolute percentage error ( $x_{MdAPE}$ ). Red corresponds to negative values of  $I$ , meaning that the performance of realistic forecasts is worse than the one attained by control rules. Blue corresponds to positive values of  $I$ , meaning that realistic forecasts outperform control rules. Each point corresponds to one of the 269 dams with  $I_{PF} > 4.7\%$ . The corresponding color represents the value of  $I$  attained via simulation with the reservoir operation model. Dams with accurate forecasts and high values of  $x_{exceed}$  (inflow frequently exceeds maximum turbine release) tend to have greater hydropower benefits realized from realistic forecasts.

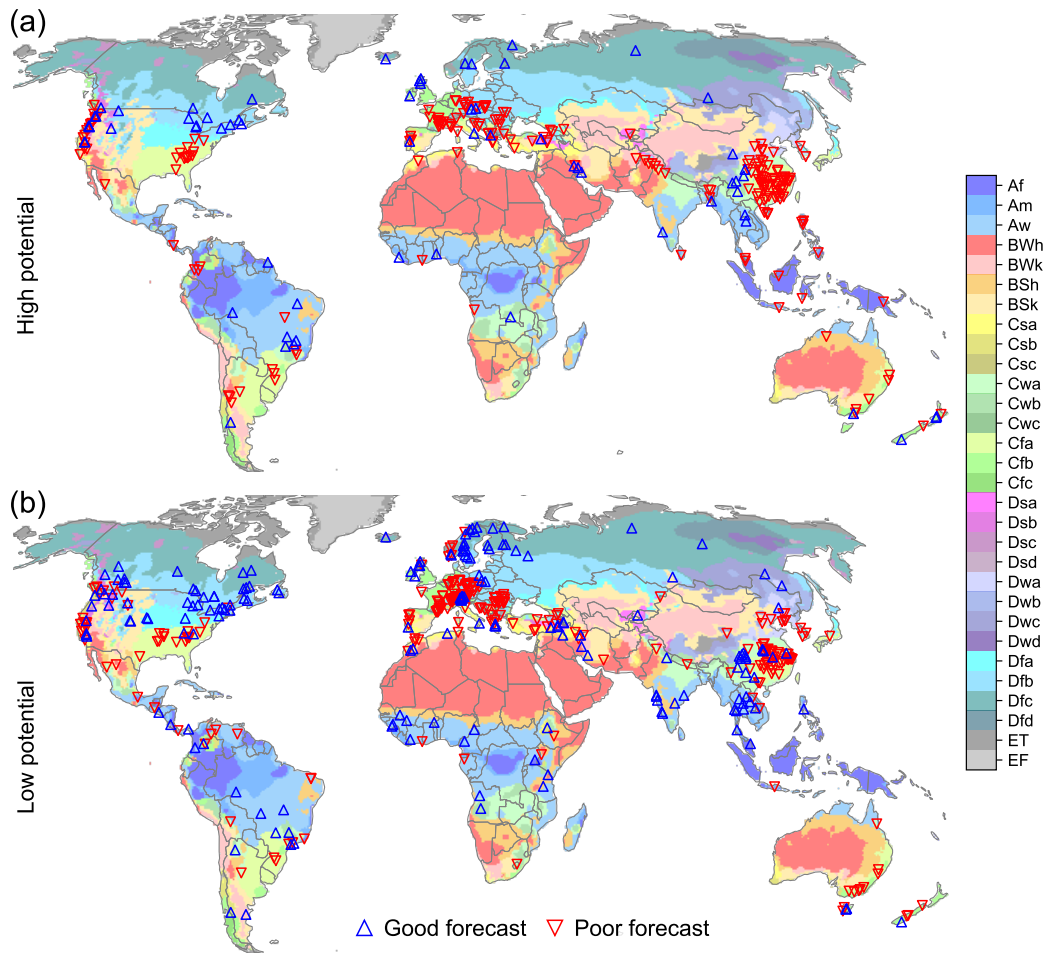


**Figure 7.** Distribution of dams across climate zones based on their potential to benefit from perfect forecasts. The top (a) and bottom (b) panels represent dams with ‘high potential’ ( $IPF > 4.7\%$ ) and ‘low potential’ ( $IPF \leq 4.7\%$ ), respectively, while ‘good forecast’ and ‘poor forecast’ represent dams with  $MdAPE$  less or greater than 20%, respectively.

**Table 1.** Coefficients of logistic regression to predict if  $I_{PF} > 4.7\%$  . The term ‘Estimate’ represents the increase in log-odds of a dam attaining *success* per unit increase in the value of the predictors.

Predictors	Estimate	Std. Error	Z-value	Pr(> z )
(Intercept)	-1.16	0.25	-4.62	<0.01
$x_{depth}$	2.84	0.31	9.25	<0.01
$x_{fill}$	-0.10	0.01	-8.76	<0.01

**Table 2.** Coefficients of linear regression to predict  $I$ .

Predictors	Estimate	Std. Error	Z-value	Pr(> z )
(Intercept)	-0.18	0.12	-1.485	0.139
$x_{MdAPE}$	-0.03	0.004	-8.554	<0.01
$x_{exceed}$	2.36	0.30	7.752	<0.01

**Table 3.** Distribution of dams across climate zones. H and L represent *high/low potential*, G and P represent *good/poor forecast*. Columns 2-5 (6-9) are the number (percentages) of dams in each group. Column 10 and 11 are the percentages of dams with *high potential* and *good forecast* respectively and are in bold if the observed frequency is different from the expected frequency (global average in final row) significantly ( $p < 0.05$  using Chi-squared test).

Climate	HG	HP	LG	LP	HG%	HP%	LG%	LP%	High%	Good%
Af	0	9	3	3	0.00	0.60	0.20	0.20	0.60	0.20
Am	4	6	5	4	0.21	0.32	0.26	0.21	0.53	0.47
Aw	7	6	26	4	0.16	0.14	0.61	0.09	0.30	<b>0.77</b>
BWh	2	2	2	0	0.33	0.33	0.33	0.00	0.67	0.67
BWk	0	3	1	0	0.00	0.75	0.25	0.00	0.75	0.25
BSh	1	2	4	6	0.08	0.15	0.31	0.46	0.23	0.39
BSk	0	2	6	5	0.00	0.15	0.46	0.39	0.15	0.46
Csa	4	11	9	19	0.09	0.26	0.21	0.44	0.35	0.30
Csb	6	15	4	10	0.17	0.43	0.11	0.29	<b>0.60</b>	0.29
Cwa	5	25	8	16	0.09	0.46	0.15	0.30	<b>0.56</b>	0.24
Cwb	1	3	7	2	0.08	0.23	0.54	0.15	0.31	0.62
Cfa	2	56	6	58	0.02	0.46	0.05	0.48	<b>0.48</b>	<b>0.07</b>
Cfb	9	15	9	41	0.12	0.20	0.12	0.55	0.33	0.24
Dsa	0	2	1	2	0.00	0.40	0.20	0.40	0.40	0.20
Dsb	2	3	5	4	0.14	0.21	0.36	0.29	0.36	0.50
Dsc	0	1	1	1	0.00	0.33	0.33	0.33	0.33	0.33
Dwa	0	5	1	8	0.00	0.36	0.07	0.57	0.36	0.07
Dwb	1	1	2	1	0.20	0.20	0.40	0.20	0.40	0.60
Dwc	2	1	2	0	0.40	0.20	0.40	0.00	0.60	0.80
Dfa	0	1	6	5	0.00	0.08	0.50	0.42	0.08	0.50
Dfb	13	21	32	41	0.12	0.20	0.30	0.38	0.32	0.42
Dfc	7	10	33	20	0.10	0.14	0.47	0.29	<b>0.24</b>	<b>0.57</b>
ET	1	2	7	36	0.02	0.04	0.15	0.78	<b>0.07</b>	<b>0.17</b>
Total	67	202	180	286	0.09	0.28	0.25	0.39	0.37	0.34